Published in final edited form as:
Osteoarthritis Cartilage. 2012 November ; 20(11): 1347–1356. doi:10.1016/j.joca.2012.07.002.

Structural and functional analysis of intra-articular interzone tissue in axolotl salamanders

Rebekah S. Cosden-Decker[*,§], **Melissa M. Bickett**[†], **Christian Lattermann**[†], and **James N. MacLeod**[†,*]

[*]Department of Veterinary Science, University of Kentucky, Lexington, KY, USA

[§]Translational Research Program in Pediatric Orthopaedics, Division of Orthopaedic Surgery, Department of Surgery, Children's Hospital of Philadelphia, Philadelphia, PA. USA

[†]Department of Orthopaedic Surgery, University of Kentucky, Lexington, KY, USA

Abstract

Objective—Mechanisms directing diarthrodial joint development may be useful in understanding joint pathologies and identifying new therapies. We have previously established that axolotl salamanders can fully repair large articular cartilage lesions, which may be due to the presence of an interzone-like tissue in the intra-articular space. Study objectives were to further characterize axolotl diarthrodial joint structure and determine the differentiation potential of interzone-like tissue in a skeletal microenvironment.

Design—Diarthrodial joint morphology and expression of Aggrecan, BOC, Type I Collagen, Type II Collagen, and GDF5 were examined in femorotibial joints of sexually mature (>12 months) axolotls. Joint tissue cellularity was evaluated in individuals from 2-24 months of age. Chondrogenic potential of the interzone was evaluated by placing interzone-like tissue into 4mm tibial defects.

Results—Cavitation reached completion in the femoroacetabular and humeroradial joints, but an interzone-like tissue was retained in the intraarticular space of distal limb joints. Joint tissue cellularity decreased to 7 months of age and then remained stable. Gene expression patterns of joint markers are broadly similar in developing mammals and mature axolotls. When interzone-

Address correspondence and reprint requests to: J.N. MacLeod, University of Kentucky, Department of Veterinary Science, 108 Gluck Equine Research Center, Lexington, KY 40546 United States. Tel: 1-859-218-1140; Fax: 1-859-257-8942. jnmacleod@uky.edu (J.N. Macleod).

Contributions

Rebekah Cosden-Decker: design of the study, acquisition of the data, analysis and interpretation, drafting and revising of the article and final approval.
Christian Lattermann: design of the study, analysis and interpretation, revising of the article and final approval.
Melissa Bickett: design of the study, axolotl surgeries, revising of the article and final approval. James N. Macleod: design of the study, analysis and interpretation, drafting and revising of the article and final approval.

Conflict of interest

All authors declare no conflict of interest with this work.

like tissue was transplanted into critical size skeletal defects, an accessory joint developed within the defect site.

Conclusions—These experiments indicate that mature axolotl diarthrodial joints are phenotypically similar to developing synovial joints in mammals. Generation of an accessory joint by interzone-like tissue suggests multipotent cellular differentiation potential similar to that of interzone cells in the mammalian fetus. The data support the axolotl as a novel vertebrate model for joint development and repair.

Keywords

Joint development; articular cartilage repair; amphibian; joint interzone; axolotl salamander

INTRODUCTION

In vertebrate organisms, the skeletal system is fundamental to maintaining physical structure and enabling motion. Relative movement and locomotion are achieved through the exertion of force across diarthroidial joints by skeletal muscle contraction, with normal structural and biomechanical properties of articular cartilage being essential for pain-free movement. Although injury and structural damage to articular cartilage can result in substantial disability in humans and other mammals, joint surface lesions have only a very limited intrinsic capacity for repair. The tissue that forms in joint surface lesions over time is a biomechanically inferior fibrocartilage that fails to restore normal surface architecture[1, 2]. A few publications have reported that cartilage lesions created in mammals *in utero* can heal without scar formation[3, 4]. Unfortunately, this apparent ability is lost after birth, such that postnatal articular lesions frequently result in chronic chondral and osteochondral defects. While they may be clinically treated with costly and extensive restorative options, such lesions eventually lead to osteoarthritis. However, there is increasing evidence that knowledge of the molecular, cellular, and tissue mechanisms directing joint development and articular cartilage maturation have the potential to contribute novel insights to efforts aimed at cartilage repair[5].

A promising, yet underutilized, model for vertebrate joint development and repair is found in *Ambystoma mexicanum*, or the Mexican axolotl mole salamander. Axolotls retain the ability to regenerate any of their four, well-defined limbs throughout their lifespan and have served as a popular model for complete limb regeneration following amputation over the last century. Despite their remarkable regenerative capacities, intrinsic skeletal repair mechanisms in axolotls have many similarities to mammals. For example, axolotls can heal simple bone fractures, but are unable to repair large bone defects in absence of amputation and blastema formation[6, 7]. Interestingly, however, we have discovered that mature axolotls possess the impressive intrinsic ability to repair large cartilage defects involving the joint surface[8]. The data also suggested that an “interzone-like” tissue occupying the intraarticular space of the femorotibial joint in axolotl salamanders serves as a source of cells contributing to articular cartilage repair. In the mammalian embryo, condensation of the prechondrogenic mesenchyme gives rise to a region of flattened cells at putative joint sites[9-12]. This area is known as the joint interzone, and lineage tracing experiments have revealed that a population of GDF5 expressing cells within the interzone gives rise to articular

chondrocytes, synovial lining, and other joint tissues[13]. While the mammalian interzone disappears with the progression of joint cavitation, an interzone-like tissue appears to persist in at least some diarthrodial joints of adult axolotls[8]. Maintenance of larval or juvenile characteristics is not limited to axolotl skeletal structures, as they display many other paedomorphic characteristics including external gills and fins throughout their lifespan. Unlike other urodele amphibians, the axolotl does not spontaneously undergo metamorphosis to a terrestrial adult form, but rather retains larval characteristics into sexually maturity[14, 15].

Although our previous research has identified axolotl interzone-like tissue as a potential source of cells contributing to articular cartilage repair, little is known about characteristics of the axolotl interzone-like tissue or its differentiation capacity. The objectives of the current study were to characterize morphological properties of this tissue during axolotl maturation and to investigate its functional capacities using a critical size defect bone fracture model. We hypothesized that the axolotl's interzone-like tissue shares structural and functional characteristics with the interzone found in fetal mammals during diarthrodial joint development. An understanding of the molecular and cellular mechanisms involved in joint formation may be very useful in gaining new insight into the etiology and pathogenesis of both developmental and acquired joint diseases. In addition, such information could enable novel therapeutic strategies aimed at restoring genuine hyaline articular cartilage.

Materials and Methods

Animal housing and care

Axolotl salamanders (*A. mexicanum*) were obtained from the Ambystoma Genetic Stock Center (Lexington, KY) as fertilized embryos. Axolotls were housed individually at 20-22°C in 25% Holtfreter's solution[16]. Larvae were fed freshly hatched brine shrimp (Artemia sp., Aquatic Ecosystems, Apopka, FL) until they reached 4 cm in length at approximately 3 months of age, after which they were fed California blackworms (*Lumbriculus* sp., J.F. Enterprises, Oakdale, CA). All procedures were conducted in accordance with a University of Kentucky institutional animal care and use protocol (IACUC #2008-0282). Prior to tissue collection, salamanders were deeply anaesthetized with 0.01% benzocaine and euthanasia was performed by cervical dislocation.

Joint Morphology, Histology, and Immunohistochemistry

A survey of axolotl appendicular joint structure was conducted using intact limbs harvested from individuals at 2 (n=2), 4 (n=4), 5 (n=5), 6 (n=6), 7 (n=5), 8 (n=3), 12 (n=4), 14 (n=2), 15 (n=1) 18 (n=4), and 24 (n=4) months of age. All limbs were fixed in 4% paraformaldehyde in PBS for 48 hours.

Alcian Blue/Alizarin Red double staining of bone and cartilage was performed as described previously[17, 18]. Briefly, limbs were dehydrated through increasing concentrations of ethanol after fixation and then transferred into Alcian Blue solution until the cartilage appeared blue. After Alcian staining, limbs were rehydrated through alcohol and remaining pigment was removed by incubation in a solution containing hydrogen peroxide. Limbs

were enzymatically digested in trypsin, stained with Alizarin Red and cleared in 0.05% potassium hydroxide and glycerin.

Limbs processed for histological analysis were decalcified in EDTA and hydrochloric acid (Richard Allen Scientific, Kalamazoo, MI) and paraffin embedded. Samples were sectioned at 7 μm. Hematoxylin and Eosin (H&E) staining was performed using standard protocols. Safranin-O/Fast Green staining was optimized and standardized for axolotl samples using aqueous 0.001% Fast Green and 0.05% Safranin-O solutions.

Immunohistochemistry was used to evaluate expression of Aggrecan, Brother of CDO (BOC), Type I Collagen, Type II Collagen, Growth/differentiation factor 5 (GDF5), and green fluorescent protein (GFP). Immunostaining was performed using standard avidin biotin complex reagents and methods according to the manufacturer's protocol (Santa Cruz Biotechnology, Cat. #sc2017, sc2019, Santa Cruz, CA). All sections were pretreated with 3% hydrogen peroxide to quench endogenous peroxidase activity. Sections stained for aggrecan, type I collagen, GDF5, and GFP were pretreated to enhance antigen retrieval with a 0.2M sodium citrate buffer, pH 3.5, for 20 minutes at 37°C. Polyclonal rabbit anti-mouse aggrecan IgG (Millipore, Cat. #AB1031, Billerica, MA) was diluted at 1:800. Polyclonal rabbit anti-rat collagen I IgG (Millipore, Cat. #AB755P, Billerica, MA) was diluted at 1:100. Polyclonal goat anti-mouse GDF5 (R&D Systems, Cat# AF853, Minneapolis, MN) was diluted at 1:250. Polyclonal rabbit anti GFP IgG (Abcam Cat. #AB290, Cambridge, MA) was diluted at 1:1500. Type II collagen and BOC stained sections were pretreated to enhance antigen retrieval with 1% pepsin in 10mM HCl for 10 minutes at 37°C. Monoclonal mouse anti-chicken collagen II IgG (Millipore, Cat. #MAB8887) was diluted at 1:800. Monoclonal mouse anti-human BOC (R&D Systems Inc., Minneapolis, MN, #MAB20361) was diluted at 1:50. All sections were counterstained with Gill No.3 hematoxylin (Sigma, Cat#HS316). Murine and equine tissues were used as positive controls for aggrecan, BOC, type I collagen, type II collagen and GDF5 immunostaining, using the same hybridization reagents and protocols. Limb sections from GFP transgenic salamanders were used as positive controls for the GFP antibody. Negative controls for each assay included omission of the primary or secondary antibody from the immunostaining protocol (Supplemental Figure 1).

Analysis of joint tissue cellularity

Cell density and tissue morphology were evaluated in femorotibial joint interzone and epiphyseal/articular cartilage of axolotls 2-24 months of age to assess age-dependent changes during maturation and adulthood. Digital images of H&E stained interzone tissue (20x magnification) and distal femoral epiphyseal/articular cartilage (4x magnification) were analyzed using CellC and MatLab software (The Mathworks, Natick, MA)[19]. After a parametric one-way ANOVA, Tukey-Kramer analysis was performed to allow for comparison of unequally sized groups at each month of age. Analyses were performed using the SAS statistical program, version 9.1 software (Statistical Analysis System, SAS Institute, Cary, NC, USA). Differences were considered significant at $p < 0.05$.

Differentiation potential of axolotl interzone-like tissue

Functional properties of axolotl interzone-like tissue were investigated with a differentiation assay in an *in vivo* skeletal microenvironment. Interzone tissue was surgically harvested from the femorotibial joint of donor individuals and placed into 4 mm defects in the tibial diaphysis of recipients. For all procedures, a surgical plane of anesthesia was achieved by immersion in 0.01% benzocaine (w/v, Sigma, Cat. #E1501, St. Louis, MO) in Holtfreter's solution. Anesthesia was maintained by wrapping the animals in a towel soaked in the same benzocaine solution throughout the procedure.

For fracture procedures, a 5-6 mm skin incision centered over the tibia was made in the left hind limb of axolotls at 7-12 months of age. The tibia was exposed by blunt dissection of surrounding soft tissues using microforceps. Simple transverse fractures of the tibia (n=12) were created using surgical scissors to make a complete cut of the bone at approximately the mid-diaphysis. Critical size bone defects (CSD) were made (n=54) by excision of a 4 mm mid-diaphyseal section of tibia (Figure 1, Supplemental Table 1). Surgical calipers were used to measure the correct bone size for removal (Fargo Enterprises Cat#784EC, Vacaville, CA). In the CSD only (no tissue transplant) group (n=12), the skin incision was closed with 10-0 vicryl suture (Coviden, Cat. #N2736K, Mansfield, MA) immediately after excision of bone. In the CSD tissue transplant experimental groups, 3 mm × 3mm sections of skin (n=13), muscle (n=12), or 3 mm × 1 mm interzone-like tissue (n=17) were harvested from germline GFP transgenic salamanders at 12-14 months of age and placed with random orientation into the tibial defect site[20] prior to suturing. Harvest of interzone-like tissue from the femorotibial joints of GFP transgenic salamanders was performed under a dissection microscope, with careful attention towards removing any attached articular cartilage. After surgery, salamanders were recovered from anesthesia in Holtfreter's solution. Limbs were collected at 15 days, 6 weeks, and 7 months after the bone defect surgery.

RESULTS

Joint Morphology

Cavitation—In Axolotls greater than 12 months of age, the hip, shoulder, and elbow joints are cavitated (Figure 2 B, C, E, F). These joints have evidence of a distinct articular surface and joint capsule. In contrast, interzone-like tissue was present in the radiocarpal and distal joints on the forelimb, and the femorotibial and distal joints on the hindlimb. (Figure 2 H, I, K, L).

Cell morphology—At earlier ages (2-4 months), the appendicular skeleton appeared entirely cartilaginous. Chondrocytes within the epiphysis and metaphysis of long bones had a similar morphology, while those in the diaphysis were larger with a more spherical appearance (Figure 3 A, B). The interzone-like tissue consisted of large, closely spaced, and flattened cells with a limited extracellular matrix (Figure 3 F, G). At 7 and 12 months of age, a medullary cavity filled primarily with adipose tissue was observed along the length of the diaphysis with a rim of cortical bone extending over a cartilaginous tissue core of the metaphysis. There was a clear distinction in chondrocyte morphology between the metaphysis and epiphysis, with those in the metaphysis appearing larger and more rounded

than those within the epiphysis (Figure 3 C, D). The interzone-like tissue also changed with maturation and developed a greater amount of extracellular matrix (Figure 3, H). At 12 and 24 months of age, two distinct interzone cell morphologies were observed, either oblong with a prominent nucleus or more rounded and chondrocyte-like (Figure 3 I, J). Chondrocytes in the oldest age group examined, 24 months, had three morphological groups (Figure 3 E). Epiphyseal/articular chondrocytes were the smallest, 10-20μM in diameter, and homogenously distributed in the extracellular matrix. Metaphyseal chondrocytes closer to the epiphysis were larger, 25-35 μM in diameter, and in clusters. Metaphyseal chondrocytes closest to the medullary cavity within the diaphysis were similar in size, but with less distinct clustering.

Joint Tissue Cellularity—Cellularity decreased in both the distal femoral epiphyseal/articular cartilage and interzone-like tissue during maturation. Cell density was highest at 2 months of age and declined in both tissues until plateauing at approximately 7 months of age. At all time points evaluated after 7 months of age, there was no difference in cellularity ($P>0.05$) (Figure 4).

Expression of joint markers—Type I collagen expression was observed in the interzone-like tissue and cortical bone (Figure 5 A,F). Immunostaining of type II collagen indicated uniform expression throughout the epiphyseal/articular cartilage. There was a marked decrease in type II collagen staining above the epiphyseal/metaphyseal junction (Figure 5 B,G). Positive immunostaining for aggrecan was present in the epiphyseal articular cartilage near the articular surface, but absent in the interzone. (Figure 5 C, H). However, a broader assessment of total proteoglycan using Safranin-O/fast green staining indicated high levels throughout the metaphyseal and epiphyseal cartilage matrix (Figure 5 D,I). BOC expression was present in both interzone and epiphyseal/articular cartilage (Figure 5 E). Round, chondrocyte-like cells within the interzone were GDF5 positive, while oblong cells appeared GDF5 negative (Figure 5 J).

Differentiation potential of axolotl interzone-like cells

Hind limb anatomy—Both the tibia and fibula of the axolotl articulate directly with the distal femur and have a similar overall size and shape. Alcian Blue and Alizarin Red staining indicate that the diaphysis is composed of mineralized bone, while the epiphysis and metaphysis are cartilaginous (Figure 6). After creation of a 4 mm critical size tibial defect, the fibula was left intact to support the limb and maintain the length of the defect site (Hutchison et al., 2007). This worked well in a majority of individuals without postoperative complications. However, bowing of the fibula occurred in four axolotls (4/54) that decreased the tibial defect length to less than 2mm at the time of collection (Supplemental Figure 2). This was seen in CSD with interzone (n=1), skin (n=1), and muscle (n=2) transplants. These samples were excluded from further analyses, as defect lengths were reduced to below the “critical size” threshold and demonstrated evidence of spontaneous repair.

Transverse fracture and critical size defect repair—Fracture size and location was confirmed at 15 days (Figure 6 A,D,G). By 6 weeks, there was evidence of cartilaginous callus formation at transverse fracture sites (Figure 6 B). At 7 months, repair at transverse

fracture sites was complete with bone remodeling underway (Figure 6 C). In contrast, there was no evidence of CSD repair in the control group at any post-surgical collection time point (Figure 6 D-F). Proximal and distal ends of the tibia at the fracture sites became rounded with some cartilage (similar to the muscle and skin transplant samples reported below, see Supplemental Figure 3), but failed to bridge the diaphyseal defect.

While 4 mm CSDs did not heal spontaneously in the axolotl, the impact of transplanted muscle, skin, and interzone-like tissue on repair was also investigated. At 15 days, cells within interzone-like tissue transplants started to display a chondrocyte-like morphology (data not shown). Columns of proteoglycan expressing tissue extended nearly the length of the defect site by 6 weeks (Figure 6 H), and by 7 months a structure that appeared cartilaginous by Alcian Blue staining filled the CSD (Figure 6 I). While none of the skin or muscle transplants repaired the defect with the exception of 3 samples with fibula bowing (Supplemental Figure 2), all of the biological replicates in the interzone transplant group achieved CSD bridging by 7 months.

Histological analysis of the interzone tissue CSD repair revealed formation of an additional or accessory joint (Figure 7). These accessory joints appeared to contain all of the tissue types found in a normal femorotibial joint, specifically an interzone-like tissue between two cartilaginous structures that displayed morphological features similar to epiphyseal/articular chondrocytes and metaphyseal chondrocytes (Figure 7 C). In addition, cells within the accessory joints were positive for GFP by immunostaining, confirming that they were derived from the interzone tissue transplants collected from transgenic GFP donors (Figure 7 D). The location of GFP-expressing cells appeared limited to accessory joint structures, with no evidence that transplanted cells migrated or proliferated outside of the tibial defect site. Skin and muscle transplants also maintained GFP expression at 7 months, but neither changes in cellular morphology nor an increase in transplant size were observed.

DISCUSSION

We have previously reported that the axolotl may be able to achieve full repair of large articular cartilage defects due to the presence of an interzone-like tissue in mature knee joints[8]. Results of the current study support our hypothesis that this interzone-like tissue is indeed similar to fetal mammalian interzone tissue and harbors multipotent differentiation potential, which likely allows it to contribute to joint repair. In developing mammals, a population of GDF5 expressing cells within the interzone gives rise to all synovial joint tissues including articular cartilage, ligaments, and synovium[13]. Our research suggests that axolotl interzone-like tissue shares many structural similarities to fetal mammalian interzone, and that it maintains its ability to differentiate into multiple joint tissues during development as well as in response to skeletal injury[8].

While mammalian joint development occurs *in utero*, axolotl limbs develop after hatching. In axolotls between 2-4 months of age, regions of flattened, elongated cells are observed at future joint sites within the cartilaginous anlagen of developing limbs. This process appears quite similar to limb development in the mammalian fetus, where joint formation continues to cavitation. The cavitation process and disappearance of the interzone tissue progresses in

a proximal to distal manner and is completed before birth in mammals. Although proximal joints in both thoracic and pelvic limbs of axolotls appear cavitated as in mammals, more distal joints do not cavitate and maintain an interzone-like tissue through at least 24 months of age. This axolotl interzone tissue appears to be structurally and functionally homologous to that found transiently during mammalian synovial joint development. While mammalian interzone tissue disappears with the progression of joint cavitation, analysis of the axolotl femorotibial joint revealed that cellularity remains constant after 7 months of age. Despite the presence of this interzone tissue, all limb joints appear to articulate freely with a wide range of motion upon physical manipulation.

In mammals, regions of flattened interzone cells switch from type II to type I collagen expression at the onset of joint formation [21, 22]. In axolotls greater than 12 months of age, type I collagen expression is also present in the interzone and type II collagen expression is seen throughout the adjacent epiphyseal/articular cartilage.

Cell density of the axolotl interzone tissue is much greater than in the adjacent articular cartilage, suggesting higher rates of cell proliferation and/or less extracellular matrix production than by chondrocytes[11]. Neither mammalian nor axolotl interzone cells produce aggrecan, and loss of this stiff proteoglycan may result in a passive “flattening” of interzone cells and associated extracellular matrix due to mechanical forces[11]. As mammalian joint development progresses, some cells within the interzone develop a more rounded shape. These rounded cells are likely associated with chondrogenesis, eventually becoming articular chondrocytes[22-24]. Interestingly, a sub-population of rounded cells was also observed within the axolotl interzone-like tissue. These rounded cells appear to have higher levels of type II collagen and GDF5, a chondrogenic factor strongly expressed in the mammalian interzone at the onset of joint formation[25, 26]. With progression of chondrocytic differentiation, mammalian interzone cells cease GDF5 expression and begin to express type II collagen[13]. Elongated, flattened cells within the axolotl interzone appear to have less or even an absence of GDF5 and type II collagen expression, suggesting that there are two functionally distinct cell populations within the axolotl interzone.

Brother of CDO (BOC) is a cell surface receptor whose expression pattern was found to be highly restricted to articular cartilage in adult mammals[27]. Although its functional role in mature articular cartilage is not yet clear, previous studies have demonstrated that BOC binds to hedgehog ligands with high affinity[28]. As in fetal mice[29], BOC expression in the axolotl was found in the interzone and adjacent cartilage.

Although the cellular density of joint tissues does not change after 7 months of age in the axolotl, skeletal growth continues to occur. A primary center of ossification is visible within the diaphyseal cartilage of young axolotls (2-4 months). At later time points, this develops into a circumferential layer of cortical bone that surrounds a medullary cavity filled with adipose tissue. The absence of secondary centers of ossification and growth plates suggests that chondrocytes within the metaphyseal and epiphyseal/articular cartilage of axolotls likely contribute to linear bone growth[30]. After 12 months of age, round GDF5 positive cells within the axolotl interzone often appear to be organized into distinct columns. The mammalian ‘articular growth plate’ model proposed by Hunziker, et al.[31] suggests that

similarly organized cells within articular cartilage contribute to expansion and growth of the articular cartilage surface. In the axolotl, these columns of cells often appear to be intimately associated with the articular surface, suggesting movement from the interzone into the articular cartilage.

After creation of a transverse tibial fracture in the axolotl, there was clear evidence of cartilaginous callus formation by 6 weeks and new bone tissue by 7 months. These events appear to parallel processes of transverse fracture repair in mammals The minimum critical dimension of a bone defect which will result in non-union fracture repair is bone- and species-specific, but this phenomenon also appears to be conserved between mammals and axolotls[32]. The current results confirm that tibial defects measuring 4 mm in length do not repair spontaneously in the axolotl, supporting previous experiments from other laboratories demonstrating that axolotls lack the intrinsic ability to repair bone defects of critical dimension[6, 7]. On the surface, this might seem surprising considering that the axolotl can regenerate an entire limb after amputation. However, in absence of limb amputation and blastema formation, intrinsic fracture repair in salamanders occurs independent of regeneration processes[6]. These data imply partial conservation of repair mechanisms between the species. Examining divergence of these mechanisms may help us to understand pathways that have been lost or are no longer utilized in mammals, but may be important for intrinsic tissue (i.e. cartilage) repair.

Failure of spontaneous CSD repair in the axolotl creates an interesting *in vivo* model within a skeletal microenvironment to study the differentiation potential of interzone-like tissue. We previously reported that the intraarticular presence of interzone-like tissue may be responsible for the remarkable intrinsic ability of axolotls to heal large femorotibial articular cartilage defects[8]. Thus, the ability of transplanted interzone to give rise to cartilaginous tissue in a tibial CSD might have been predicted. However, the current data indicate that interzone cells are not limited to an articular chondrocyte fate, but instead have the potential to differentiate into all of the cell types normally found in axolotl diarthrodial joints, including articular/epiphyseal cartilage, metaphyseal cartilage, and interzone. This indicates that these cells are indeed multipotent, a characteristic which is shared with interzone cells of developing mammalian joints[13].

Restoration of damaged articular cartilage is an enormous challenge for patients and clinicians alike. We have now described a vertebrate model organism that is able to fully repair articular cartilage as well as construct entirely new joints from an existing population of cells. This process is different from blastema-dependent regeneration, and may provide insight into molecular and cell-based skeletal repair mechanisms with therapeutic potential for mammalian patients. Similar insights gained from developmental biology research are currently being used to test cell reprogramming strategies in other fields, but have not yet been realized in skeletal medicine[33-35].

Supplementary Material

Refer to Web version on PubMed Central for supplementary material.

Acknowledgments

Assistance with image analysis from Dr. Jinze Liu and Jizhou Gao are graciously acknowledged.

Role of funding source:

Financial support was received from the Kentucky Equine Drug Research Council, the Lourie Foundation, the Gluck Equine Research Center, and the University of Kentucky Department of Orthopaedic Surgery. Dr. Christian Lattermann is currently supported by a University of Kentucky Physician Scientist Development Award and by a NIH-NIAMS K-23 AR060275-01A1.These study sponsors were not involved in the study design, data collection or analysis; or in the writing of the manuscript. Furthermore, they did not affect the decision to submit the manuscript for publication.

References

1. Riddle WE Jr. Healing of articular cartilage in the horse. J Am Vet Med Assoc. 1970; 157:1471–1479. [PubMed: 4922186]
2. Shapiro F, Koide S, Glimcher MJ. Cell origin and differentiation in the repair of full-thickness defects of articular cartilage. J Bone Joint Surg Am. 1993; 75:532–553. [PubMed: 8478382]
3. Calandruccio RA, Gilmer WSJR. Proliferation, Regeneration, and Repair of Articular Cartilage of Immature Animals. J Bone Joint Surg Am. 1962; 44:431–455.
4. Namba RS, Meuli M, Sullivan KM, Le AX, Adzick NS. Spontaneous repair of superficial defects in articular cartilage in a fetal lamb model. J Bone Joint Surg Am. 1998; 80:4. [PubMed: 9469302]
5. Pitsillides AA, Beier F. Cartilage biology in osteoarthritis[mdash]lessons from developmental biology. Nat Rev Rheumatol. 2011; 7:654–663. [PubMed: 21947178]
6. Satoh A, Cummings GM, Bryant SV, Gardiner DM. Neurotrophic regulation of fibroblast dedifferentiation during limb skeletal regeneration in the axolotl (Ambystoma mexicanum). Dev Biol. 2010; 337:444–457. [PubMed: 19944088]
7. Hutchison C, Pilote M, Roy S. The axolotl limb: a model for bone development, regeneration and fracture healing. Bone. 2007; 40:45–56. [PubMed: 16920050]
8. Cosden RS, Lattermann C, Romine S, Gao J, Voss SR, MacLeod JN. Intrinsic repair of full-thickness articular cartilage defects in the axolotl salamander. Osteoarthritis Cartilage. 2011; 19:200–205. [PubMed: 21115129]
9. Holder N. An experimental investigation into the early development of the chick elbow joint. J Embryol Exp Morphol. 1977; 39:115–127. [PubMed: 886251]
10. Mitrovic D. Development of the diarthrodial joints in the rat embryo. Am J Anat. 1978; 151:475–485. [PubMed: 645613]
11. Craig FM, Bentley G, Archer CW. The spatial and temporal pattern of collagens I and II and keratan sulphate in the developing chick metatarsophalangeal joint. Development. 1987; 99:383–391. [PubMed: 2958266]
12. Nalin AM, Greenlee TK Jr, Sandell LJ. Collagen gene expression during development of avian synovial joints: transient expression of types II and XI collagen genes in the joint capsule. Dev Dyn. 1995; 203:352–362. [PubMed: 8589432]
13. Koyama E, Shibukawa Y, Nagayama M, Sugito H, Young B, Yuasa T, et al. A distinct cohort of progenitor cells participates in synovial joint and articular cartilage formation during mouse limb skeletogenesis. Dev Bio. 2008; 316:62–73. [PubMed: 18295755]
14. Gould, SJ. Ontogeny and phylogeny. Belknap press; 1977.
15. Shaffer HB. Evolution in a paedomorphic lineage. II. Allometry and form in the Mexican ambystomatid salamanders. Evolution. 1984; 38:1207–1218.
16. Armstrong, J.; Duhon, S.; Malacinski, G. Raising the axolotl in captivity. Oxford University Press; USA: 1989.
17. Dingerkus G, Uhler LD. Enzyme clearing of alcian blue stained whole small vertebrates for demonstration of cartilage. Stain Technology. 1977; 52:229. [PubMed: 71769]
18. Wassersug RJ. A procedure for differential staining of cartilage and bone in whole formalin-fixed vertebrates. Biotechnic & Histochemistry. 1976; 51:131–134.

19. Selinummi J, Seppala J, Yli-Harja O, Puhakka JA. Software for quantification of labeled bacteria from digital microscope images by automated image analysis. BioTechniques. 2005; 39:859. [PubMed: 16382904]
20. Sobkow L, Epperlein H-H, Herklotz S, Straube WL, Tanaka EM. A germline GFP transgenic axolotl and its use to track cell fate: Dual origin of the fin mesenchyme during development and the fate of blood cells during regeneration. Dev Bio. 2006; 290:386–397. [PubMed: 16387293]
21. von der Mark K, Gauss V, von der Mark H, Müller P. Relationship between cell shape and type of collagen synthesised as chondrocytes lose their cartilage phenotype in culture. Nature. 1977; 267:531–532. [PubMed: 559947]
22. Benya PD, Padilla SR, Nimni ME. Independent regulation of collagen types by chondrocytes during the loss of differentiated function in culture. Cell. 1978; 15:1313–1321. [PubMed: 729001]
23. Archer CW, Rooney P, Wolpert L. Cell shape and cartilage differentiation of early chick limb bud cells in culture. Cell Diff. 1982; 11:245–251.
24. Solursh M, Linsenmayer TF, Jensen KL. Chondrogenesis from single limb mesenchyme cells. Dev Bio. 1982; 94:259–264. [PubMed: 6759202]
25. Storm EE, Kingsley DM. Joint patterning defects caused by single and double mutations in members of the bone morphogenetic protein (BMP) family. Development. 1996; 122:3969–3979. [PubMed: 9012517]
26. Buxton P, Edwards C, Archer CW, Francis-West P. Growth/Differentiation Factor-5 (GDF-5) and Skeletal Development. J Bone Joint Surg Am. 2001; 83:S1–23.
27. Vanderman KS, Tremblay M, Zhu W, Shimojo M, Mienaltowski MJ, Coleman SJ, et al. Brother of CDO (BOC) expression in equine articular cartilage. Osteoarthritis Cartilage. 2011; 19:435–438. [PubMed: 21262369]
28. Kavran JM, Ward MD, Oladosu OO, Mulepati S, Leahy DJ. All Mammalian Hedgehog Proteins Interact with Cell Adhesion Molecule, Down-regulated by Oncogenes (CDO) and Brother of CDO (BOC) in a Conserved Manner. J Bio Chem. 2010; 285:24584–24590. [PubMed: 20519495]
29. Mulieri PJ, Kang JS, Sassoon DA, Krauss RS. Expression of the boc gene during murine embryogenesis. Dev Dyn. 2002; 223:379–388. [PubMed: 11891987]
30. Hanken J. Appendicular skeletal morphology in minute salamanders, genus Thorius (Amphibia: Plethodontidae): growth regulation, adult size determination, and natural variation. J Morph. 1982; 174:57–77.
31. Hunziker EB, Kapfinger E, Geiss J. The structural architecture of adult mammalian articular cartilage evolves by a synchronized process of tissue resorption and neoformation during postnatal development. Osteoarthritis and Cartilage. 2007; 15:403–413. [PubMed: 17098451]
32. Schmitz J, Hollinger J. The critical size defect as an experimental model for craniomandibulofacial nonunions. Clin Orthop Relat Res. 1986; 205:299. [PubMed: 3084153]
33. Nicholas CR, Kriegstein AR. Regenerative medicine: Cell reprogramming gets direct. Nature. 2010; 463:1031–1032. [PubMed: 20182502]
34. Szabo E, Rampalli S, Risueno RM, Schnerch A, Mitchell R, Fiebig-Comyn A, et al. Direct conversion of human fibroblasts to multilineage blood progenitors. Nature. 2010; 468:521–526. [PubMed: 21057492]
35. Zhou Q, Melton DA. Extreme makeover: converting one cell into another. Cell Stem Cell. 2008; 3:382–388. [PubMed: 18940730]
36. Hall, BK. Fins into limbs: evolution, development, and transformation. University of Chicago Press; USA: 2007.

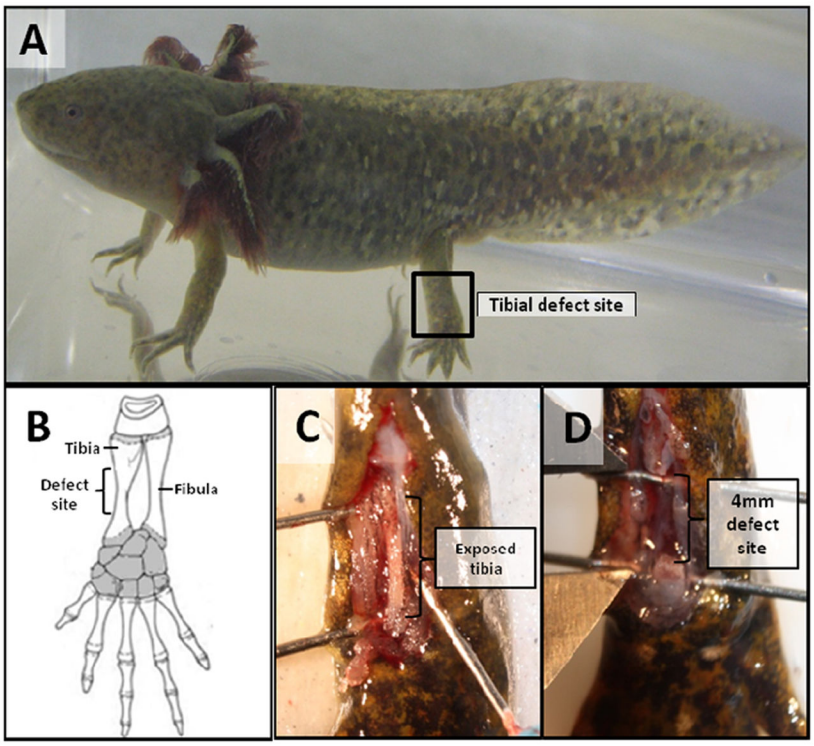

Figure 1. Tibial defect model in the axolotl salamander

(A) Tibial defect location and (B) hind limb anatomy schematic, adapted from Hall, 2007[36]. (C) Surgical exposure of the tibia diaphysis prior to gap fracture creation. (D) The critical size tibial defects were made by removing a 4 mm length of tibial diaphysis.

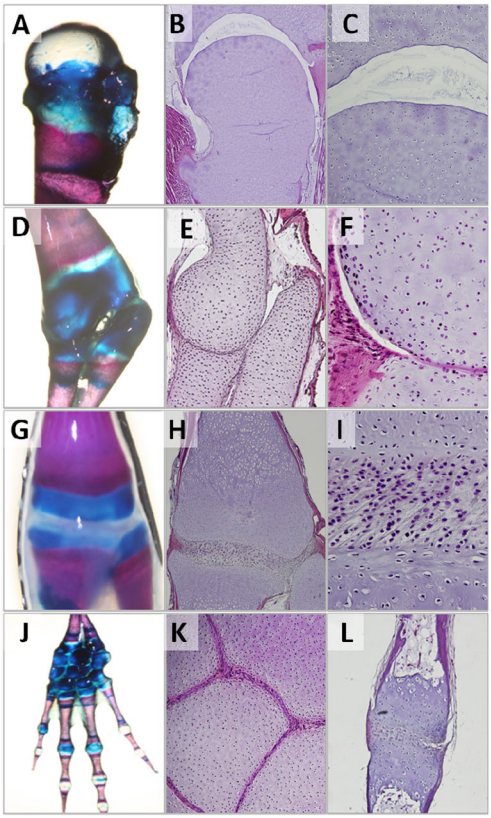

Figure 2. Diarthrodial joint anatomy in axolotls greater than 12 months of age

Whole mount Aliziran Red and Alician Blue double staining of cartilage and bone structures in the (A) proximal femur, (D) radiohumoral, (G) femorotibial, and (J) carpal-metacarpal-phalangeal structures. Histological analyses reveal that cavitation occurs in the more proximal joints including femoroacetabular (B,C) and radiohumoral (E,F) articulations, while an interzone-like tissue is retained in more distal joints including the femorotibial (H,I), metacarpophalangeal (K), and interphalangeal (L) articulations.

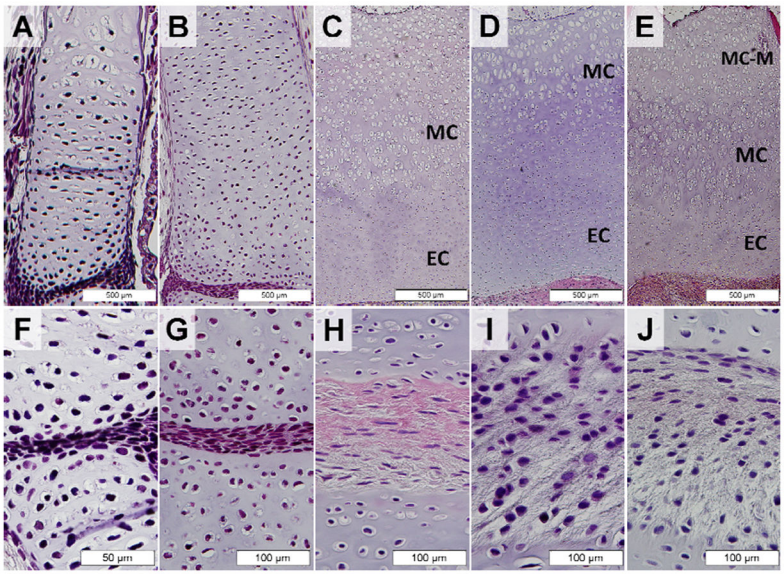

Figure 3. Changes in cell morphology of tissue within the axolotl femorotibial joint from 2-24 months of age

Distal femoral cartilage (A-E) and interzone-like tissue of axolotl salamanders at 2, 4, 7, 12 and 24 months of age (F-J). Scale bar lengths are indicated. EC, epiphyseal/articular cartilage. MC, metaphyseal cartilage. MC-M, morphologically distinct metaphyseal cartilage zone adjacent to the medullary cavity.

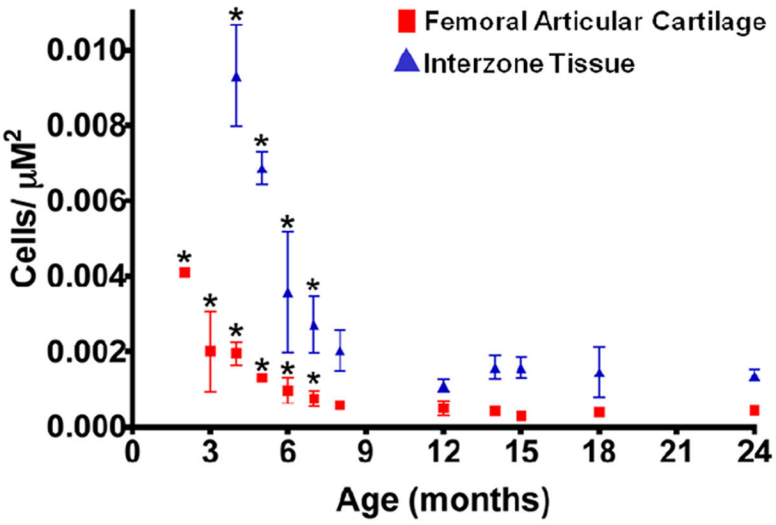

Figure 4. Changes in cellularity of axolotl epiphyseal/articular cartilage in the distal femur and interzone-like tissue in the femorotibial joint from 2-24 months of age (mean±SD)

*Denotes difference in cellularity from groups after 7 months of age (P<;0.05).

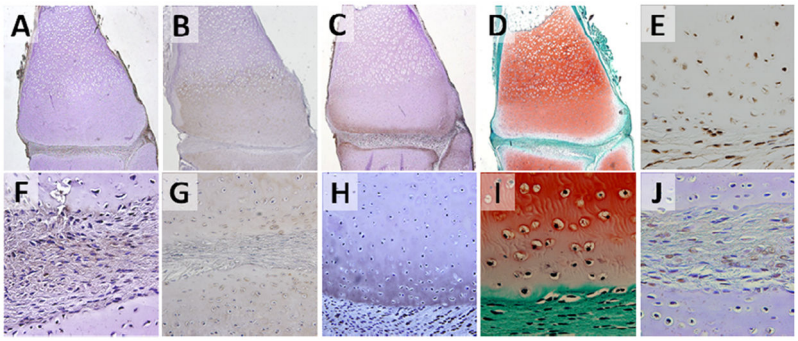

Figure 5. Expression of joint markers in mature axolotls

Type I collagen (A, F), type II collagen (B,G), Aggrecan (C,H), Proteoglycans (D,I), BOC (E) and GDF-5 (J) in the distal femoral cartilage and interzone-like tissue of axolotl salamanders at greater than 12 months of age. Type I collagen, type II collagen, aggrecan, BOC, and GDF-5 were detected by immunohistochemistry. Proteoglycan was visualized by Safranin-O staining. Images A-E are shown at 4x magnification, while images F-J are shown at 20x magnification.

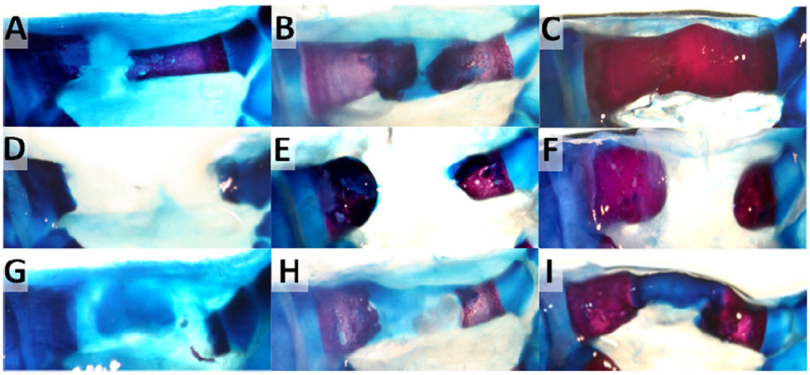

Figure 6. Tibial fracture repair in axolotl salamanders

Whole mount bone (Aliziran Red) and cartilage (Alcian Blue) staining of (A-C) transverse bone fractures, (D-F) critical size bone defects, and (G-I) critical size bone defects with interzone tissue transplant at 15 days (A,D,G), 6 weeks (B,E,H), and 7 months (C,F,I) after surgery.

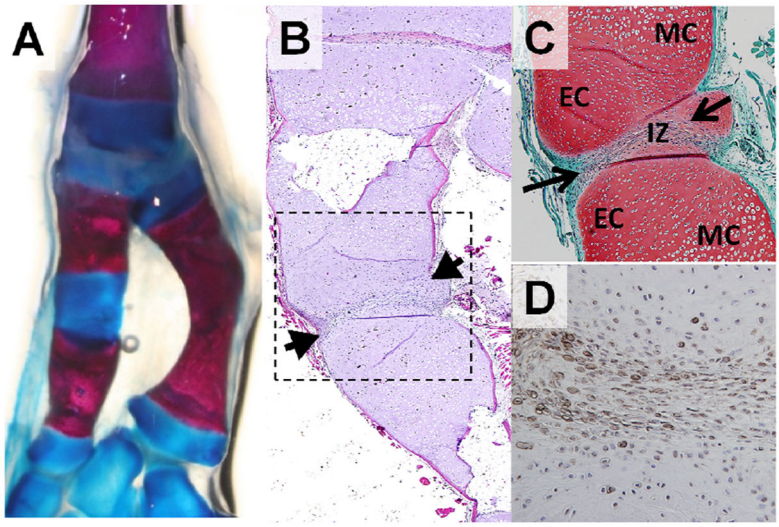

Figure 7. Repair of critical size tibial defects with interzone-like tissue transplants at 7 months post-surgery

(A) Whole mount Alcian Blue and Alizarin Red staining and (B) H&E staining reveal formation of an accessory joint (box) including interzone tissue (arrowheads) within the tibial defect space. (C) Safranin-O stained image demonstrates metaphyseal cartilage (MC), epiphyseal/articular cartilage (EC) and interzone tissue (IZ, arrows) within the accessory joint. (D) All tissues within the accessory joint displayed positive immunostaining for GFP confirming their development from the original interzone tissue transplant.